

# **Isothermal B2–B19' martensitic transformation in Ti-rich Ni–Ti shape memory alloy**

D. Salas,<sup>a,\*</sup> E. Cesari,<sup>a</sup> J. Van Humbeeck<sup>b</sup> and S. Kustov<sup>a</sup>

<sup>a</sup>Universitat de les Illes Balears, Palma de Mallorca E-07122, Spain

<sup>b</sup>Katholieke Universiteit Leuven, Leuven B-3001, Belgium

Received 20 September 2013; revised 25 October 2013; accepted 26 October 2013

Available online 4 November 2013

The athermal/isothermal nature of the B2↔B19' martensitic transformation was investigated by means of electrical resistance measurements in a Ni<sub>49.5</sub>Ti<sub>50.5</sub> alloy that has elevated transformation temperatures as compared with the near-equiatomic or Ni-rich compositions studied previously. The direct B2–B19' martensitic transformation shows a clear time dependence, whereas isothermal effects are not revealed for the reverse B19'–B2 transition. The applicability of the C-shaped time–temperature–transformation diagram to interpret the experimental results is discussed.

© 2013 Acta Materialia Inc. Published by Elsevier Ltd. All rights reserved.

**Keywords:** Shape memory alloys (SMA); Martensitic phase transformation; Phase transformation kinetics; Differential scanning calorimetry (DSC); Electrical resistivity/conductivity

Recent interest in the classical topic of isothermal martensitic transformations (MTs) [1–4] arises from results on the novel Heusler-type metamagnetic shape memory alloys, Ni–Mn–X (X = In, Sn, Sb) [5], where the direct transformation shows features typical of an isothermal martensitic transformation (IMT). Unexpected results were obtained on classical Ni–Ti shape memory alloys, which were shown to possess a clear isothermal nature [6–9]. All possible transformation paths in the Ni–Ti system of alloys have been analyzed and the conclusion has been drawn that all direct transitions to the B19' phase as well as B19'→R and B19'→B19 are isothermal, whereas the B2↔R, B2↔B19 transitions are athermal within practical experimental resolution [7]. The difference between the athermal/isothermal nature of these transformation was related to the transformation hysteresis and attributed to the complicated accommodation in the case of the transition to B19' martensite. The situation remained unclear for the B19'→B2 MT in Ni<sub>50.2</sub>Ti<sub>49.8</sub> alloy: the resistivity had a very low sensitivity to this MT, because the maximum transformation rate (heat flow maximum) vs. temperature coincided with the resistivity maximum. This situation implies insensitivity of the resistance to the variations of the martensite fraction  $\Delta F$  around the resistivity maximum.

Very recently Fukuda et al. [8] have applied resistivity measurements to study the isothermal/athermal nature of the direct and reverse MTs of the B2↔B19' MT in a Ni<sub>51.2</sub>Ti<sub>48.8</sub> alloy quenched from 1270 K, which after this heat treatment demonstrates only a partial B2↔B19' MT. Surprisingly, very strong isothermal effects were reported for the temperature near 130 K. The authors also detected certain isothermal phenomena during the reverse B19'→B2 MT and interpreted the effect of temperature on the intensity of the isothermal effects in terms of the C-shaped time–temperature–transformation (TTT)-like diagram.

The aim of the present work is twofold. We intend to verify

- whether or not the regularities relevant to the isothermal/athermal nature of B2↔B19' MT revealed for Ni-rich alloys hold in the case of the Ti-rich one;
- the effect of the increase of the MT temperature by nearly 200 K (from 130 K [8] or 160 K [7] to 330 K for the Ti-rich alloy) on the isothermal effects in the Ni–Ti system.

A Ti-rich Ni<sub>49.5</sub>Ti<sub>50.5</sub> alloy, selected for the present study, recovers the sensitivity of the resistivity to the transformed martensite fraction  $F$ : it demonstrates a monotonous increase in resistivity during the reverse B19'→B2 MT (without a maximum of  $R$  around the maximum of the transformation rate as in Ni<sub>50.2</sub>Ti<sub>49.8</sub> alloy).

\* Corresponding author. Tel.: +34 971 17 2536; e-mail: [daniel.salas@uib.es](mailto:daniel.salas@uib.es)

Therefore, previously used experimental procedures [6–8] can be applied to this system, enabling direct comparison of the data for different alloys and temperature ranges.

A  $\text{Ni}_{49.5}\text{Ti}_{50.5}$  ingot was prepared by arc-melting. The ingot was homogenized at 1470 K for 3600 s and cut using a diamond saw into samples with dimensions  $12.5 \text{ mm} \times 1.8 \text{ mm} \times 0.7 \text{ mm}$  for the resistance measurements and  $3.5 \text{ mm} \times 1.8 \text{ mm} \times 0.7 \text{ mm}$  for the differential scanning calorimetry (DSC) tests. The samples were heat treated at 920 K for 1800 s and water quenched. The four-probe method was used for resistance measurements between 300 and 390 K with a cooling/heating rate of  $2 \text{ K min}^{-1}$ . The cooling/heating rate for the DSC tests was  $10 \text{ K min}^{-1}$ .

The temperature dependences of the electrical resistance,  $R$ , are shown in Figure 1a for several temperature cycles; cycle 1 is an uninterrupted cycle, whereas cycles 2 and 3 were stopped several times at different temperatures inside the MT range to perform isothermal holding experiments: cycle 2 was interrupted during the reverse  $\text{B19}' \rightarrow \text{B2}$  MT and cycle 3 during the direct  $\text{B2} \rightarrow \text{B19}'$  MT range. Firstly, there is a substantial increase in  $R$ : between cycles 1 and 3 the resistance increases nearly 2% in austenite and 5% in martensite. Furthermore, all characteristic transformation temperatures, excluding  $A_S$ , decrease with thermal cycling—see the inset in Figure 1a. By contrast, the  $A_S$  slightly increases. Therefore, the reverse  $\text{B19}' \rightarrow \text{B2}$  MT range,  $A_F \rightarrow A_S$ , slightly decreases, whereas the transformation hysteresis increases with the number of cycles. A similar effect of thermal cycling was observed in previous studies of the  $\text{B2} \rightarrow \text{B19}'$  MT in Ni-rich Ni–Ti alloys [10,11] and in Ti-rich Ni–Ti alloys [12].

It is important for the present study to determine whether the effect of thermal cycling on MT temperatures stems from the exposure of the material to high tempera-

tures or from the martensitic transformation. To clarify this point, DSC was performed on two samples subjected to the same heat treatment. The first sample was cycled three times between 270 and 400 K, and the heat flow on cooling is shown in Figure 1b. The second sample was also subjected to three cycles within the same temperature limits; however, for this sample each cycle was interrupted on heating at 390 K (slightly above the reverse MT) for 3600 s. These data are shown in Figure 1c. The evolution of the peak temperature of the direct transformation,  $T_P$ , is shown for both samples in an inset in Figure 1c. The  $T_P$  of the first sample changes from 337.2 to 334.3 K and of the second one from 335.2 to 332.2 K. The variation of the MT temperatures of both samples is essentially the same, showing no appreciable effect of the aging at 390 K. Hence, the change in the MT temperatures is not produced by any isothermal process unrelated to the MT, such as atomic diffusion.

A comparison of the reduced temperature derivative of the resistance,  $R^{-1}(\partial R/\partial T)$ , and of the heat flow is shown in Figure 2. The  $R^{-1}(\partial R/\partial T)$  is hereinafter obtained by subtracting the baseline due to the temperature dependence of  $R$  in austenite and martensite outside the MT range. The correspondence between both curves on cooling and on heating is quite good, confirming the applicability of resistivity measurements in studying the isothermal/athermal nature of Ti-rich alloy, in contrast to the  $\text{Ni}_{50.2}\text{Ti}_{49.8}$  alloy [7].

Figure 3 shows the time dependence of the normalized resistance,  $(R(t) - R_0)/R_0$ , after interruptions of the thermal cycle at different temperatures on cooling (Fig. 3a) and on heating (Fig. 3b), with  $R_0$  being the value of  $R$  on interruption of the cooling/heating ramp. The x-axis represents the time elapsed from the moment when the temperature reaches its minimum/maximum due to the inevitable small overcooling/overheating of around 0.2 K [7] after interruption of the cycle. For clarity, only a few curves are shown for the measurements inside the transformation range. A noticeable isothermal change of  $R$  is detected on cooling at 320, 325, 330, 335 and 340 K, coinciding with the domain of the direct

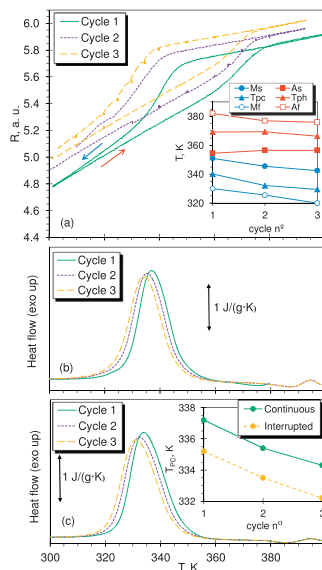


**Figure 1.** (a) Temperature dependence of the electrical resistance for a sample of  $\text{Ti}_{50.5}\text{Ni}_{49.5}$  alloy in three consecutive thermocycles: cycle 1 is non-interrupted; cycles 2 and 3 are interrupted several times on heating and cooling, respectively. The inset in (a) shows the evolution of temperatures  $M_S$ ,  $M_F$ ,  $T_{PC}$ ,  $A_S$ ,  $A_F$ ,  $T_{PH}$  along these cycles. DSC signals in three consecutive continuous (b) and interrupted (c) calorimetric scans for two different  $\text{Ti}_{50.5}\text{Ni}_{49.5}$  samples. The scans in (c) were interrupted for 3600 s at 390 K during heating. The inset in (c) shows the change of  $T_{PC}$  (in the text  $T_P$ ) through the experiments in (b) and (c).

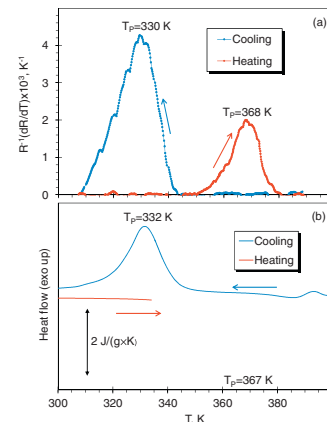


**Figure 2.** (a) Reduced temperature derivative of the electrical resistance for the  $\text{B2} \rightarrow \text{B19}'$  transformation for a sample of  $\text{Ti}_{50.5}\text{Ni}_{49.5}$  alloy. (b) DSC scan for a piece of the same sample after three thermal cycles in the resistance experiments. The  $(\partial R/\partial T)/R$  data correspond to the cycles 2 and 3 in Figure 1a where the majority of isothermal dwellings were performed.

Download English Version:

<https://daneshyari.com/en/article/1498484>

Download Persian Version:

<https://daneshyari.com/article/1498484>

[Daneshyari.com](https://daneshyari.com)